Articles in PresS. Am J Physiol Endocrinol Metab (April 4, 2017). doi:10.1152/ajpendo.00409.2016

Cyp8b1 ablation prevents western diet-induced weight gain and hepatic steatosis due to impaired fat absorption

Enrico Bertaggia[1], Kristian K. Jensen[2], Jose Castro-Perez[2], Yimeng Xu[1], Gilbert Di Paolo[1,3], Robin B. Chan[1], Liangsu Wang[2], and Rebecca A. Haeusler[1#]

[1] Columbia University Department of Pathology and Cell Biology, New York, NY, USA
[2] Merck Research Laboratories, Diabetes Department, Kenilworth, NJ, USA
[3] Denali Therapeutics Inc., South San Francisco, CA, USA
[#]Corresponding Author

Running Head: Eliminating 12α hydroxy bile acids reduces lipid absorption

Correspondence: Rebecca A. Haeusler, Russ Berrie Pavilion room 303A, 1150 St. Nicholas Ave, New York, 10032, NY, USA. Email: rah2130@cumc.columbia.edu Phone: 212-851-4899 Fax: 212-851-5335

Key Words: Bile acids; lipid absorption; obesity; diabetes; triglyceride

ABSTRACT

Bile acids (BAs) are cholesterol derivatives that regulate lipid metabolism, through their dual abilities to promote lipid absorption and activate BA receptors. However, different BA species have varying abilities to perform these functions. Eliminating 12α-hydroxy BAs in mice via *Cyp8b1* knockout causes low body weight and improved glucose tolerance. The goal of this study was to determine mechanisms of low body weight in *Cyp8b1*$^{-/-}$ mice. We challenged *Cyp8b1*$^{-/-}$ mice with western type diet and assessed body weight and composition. We measured energy expenditure, fecal calories, lipid absorption and performed lipidomic studies on feces and intestine. We investigated the requirement for dietary fat in the phenotype using a fat-free diet. *Cyp8b1*$^{-/-}$ mice were resistant to western diet-induced body weight gain, hepatic steatosis, and insulin resistance. These changes were associated with increased fecal calories, due to malabsorption of hydrolyzed dietary triglycerides. This was reversed by treating the mice with taurocholic acid, the major 12α-hydroxylated BA species. The improvements in body weight and steatosis were normalized by feeding mice a fat-free diet. The effects of BA composition on intestinal lipid handling are important for whole-body energy homeostasis. Thus, modulating BA composition is a potential tool for obesity or diabetes therapy.

INTRODUCTION

Bile acids (BAs) are amphipathic molecules synthesized in the liver from cholesterol. They are well-known for their role as surfactants, and this function is fundamental for the absorption of lipids and liposoluble vitamins upon the ingestion of a meal (8, 10, 34). Since the discovery of FXR and TGR5 as target receptors for BAs, a wealth of data has shown that BAs act as signaling molecules in various tissues throughout the body, regulating a variety of metabolic pathways (21, 24, 27, 28, 31, 41).

Two key enzymes of BA synthesis are CYP7A1 and CYP8B1. The former carries out the rate-limiting first step of BA synthesis. The latter–CYP8B1–is a BA 12α-hydroxylase that determines the production of cholic acid ([CA], which is 12α-hydroxylated) versus chenodeoxycholic acid ([CDCA], which is not). In rodents, CDCA is 6-hydroxylated soon after its synthesis into muricholic acids (MCA). Endogenously produced primary BAs can be further modified by intestinal microbes into secondary BAs, such as deoxycholic acid, which is generated from CA and is 12α-hydroxylated. Every BA species has unique physicochemical properties that can affect its interaction with BA receptors (25, 33), as well as its ability to solubilize lipids and cholesterol (40, 43).

The importance of BA composition in metabolism in humans was underscored by our finding that individuals who are very insulin sensitive have lower levels of 12α-hydroxylated BAs, whereas those who are insulin resistant have higher levels (13). These alterations are consistent with (i) the regulation of *Cyp8b1* by the insulin-repressible FOXO transcription factors (15), (ii) the increases in 12α-hydroxylated BAs in rodent models of diabetes (2, 3, 36, 37), and (iii) the observations that obese and type 2 diabetic subjects preferentially synthesize 12α-hydroxylated BAs (6, 14). Moreover, we found that low BA 12α-hydroxylation was associated with lower BMI, lower triglycerides, improvements in fatty liver, and enhanced insulin-stimulated glucose disposal (13). These findings raised the possibility that 12α-hydroxy BAs regulate metabolic homeostasis. Indeed, the absence of 12α-hydroxy BAs, as found in *Cyp8b1*$^{-/-}$

mice, has been linked to reduced cholesterol absorption (30), reduced atherosclerosis (32), as well as low body weight and improved glucose homeostasis (4, 20).

In this work we investigated the role of 12α-hydroxylated BAs in intestinal lipid absorption and the implications of this pathway on western diet-induced body weight gain. We show that ablating *Cyp8b1*, thereby eliminating 12α-hydroxylated BAs (26), leads to reduced absorption of dietary triglyceride, with intact triglyceride hydrolysis. This prevents western diet-induced body weight gain, fat accumulation, and steatosis, and improves insulin sensitivity. These alterations occur due to alterations of BA composition, not total levels, as *Cyp8b1*$^{-/-}$ mice have no decrease–and in fact a slight increase–in total BAs (26). Taken together, these data suggest CYP8B1 as a potential therapeutic target for obesity and diabetes.

MATERIALS AND METHODS

Mice and Diets–Cyp8b1$^{-/-}$ mice were generated at Taconic using a C57BL/6 background (model 11784). All the mice used in the experiments came from crossing of a heterozygous couple, in order to have control, *Cyp8b1*$^{+/-}$and *Cyp8b1*$^{-/-}$littermates. Only male mice between 8-12 weeks of age were used for the experiments.

Mice were fed standard chow diet (3.4 kcal/g, Purina 5053), western type diet (4.5 kcal/g, 42% kcal from fat and 0.2% cholesterol, TD 88137, Envigo) or fat–free diet, (3.3 kcal/g; 24.2% kcal from protein, 75.8% from carbohydrate, TD 03314, Envigo) for up to four weeks before euthanasia. Mice were housed in a 12–hour light/dark cycle. The 16-hour fast began at 6:00 pm and the refeeding at 10:00 am. Food intake measurement was obtained by mice caged individually with a food dispenser located inside the cage. Euthanasia was performed by CO2 asphyxiation followed by cervical dislocation. All experiments were conducted in accordance to Columbia University IACUC guidelines.

Gene Expression–RNA was extracted from liver using Trizol (Life Technologies), cDNA was obtained using High Capacity cDNA reverse transcription kit (Applied Biosystem). qPCR was performed with iTaq Universal SYBR green supermix (BioRad). 36b4 was used as housekeeping gene for normalization.

36b4 Fwd: AGATGCAGCAGATCCGCAT 36b4 Rev: GTTCTTGCCCATCAGCACC

Cyp8b1 Fwd: GCCCACAGCCTTCAAGTATG Cyp8b1 Rev: CGACCAGCTTGAAGTCGAAG.

Metabolic tests–The oral glucose tolerance test was performed 2 weeks after the start of western type diet (WTD) feeding. We subjected mice to a 16-h overnight fast followed by oral administration of glucose by gavage (2 g/kg). Glucose levels were assessed with OneTouch glucose monitor and strips (Lifescan). Insulin was measured using an ELISA Kit (Mercodia). Fasted glucose and insulin we measured at 10:00 am after a 16-h overnight fast. Body composition was assessed using an time-domain-NMR (Minispec Analyst AD; Bruker Optics) (16).

Lipid extraction from liver was performed as described (11). Lipids were measured using colorimetric assays: triglycerides (Infinity, Thermo Scientific) and cholesterol (Cholesterol E, Wako), and values were normalized by liver weight. Oil Red O staining was performed on snap-frozen liver sections .

For the glycogen measurement, 200 mg of liver from mice refed for 5h was homogenized in 1 ml of 6% perchloric acid and centrifuged at 18000xg for 10 min at 4°C. The supernatant was added to distilled water in a 1:1 ratio and centrifuged again. The supernatant was adjusted to pH 7.0 with KOH and centrifuged, the supernatant was incubated with amyloglucosidase (Sigma A7420, from aspergillus niger 30-60 unit/mg) at 42°C for 2 hours. Released glucose was quantified using glucose assay kit (Sigma).

Bile acid pool measurements. To measure the total BA pool, we fasted chow-fed mice for 5-hours, euthanized them, and collected the liver + gallbladder + small intestine. We doubly homogenized these tissues together in 2 volumes of 50% methanol using a rotor stator homogenizer, followed by a dounce Teflon/glass homogenizer. To 200 µl of each sample, we added deuterated bile acid standard (20 µl of 25 µM d4-cholic acid). In parallel, we generated calibrator curves of each BA measured, in charcoal-stripped tissue. To each sample/calibrator, we added 2 ml ice-cold acetonitrile, vortexed for 1 hour at 2000 rpm, and centrifuged for 10 min at 11,000xg. Supernatants were transferred to clean glass tube and dried down at 45 degrees C under nitrogen. We then extracted each sample/calibrator a second time in 1 ml of ice cold acetonitrile, vortexed for 1 hour at 2000 rpm, centrifuged 10 min at 11,000xg. The supernatant of the second extraction was combined with the first, and dried down at 45 degrees C under nitrogen. We

112 resuspended each sample in 200µl of 55/45 (v/v) methanol/water both with 5mM ammonium formate.
113 Samples were spun in UltraFree MC 0.2µm centrifugal filters (Millipore), transferred to LC/MS vials, and
114 10µl were injected into UPLC-MS/MS (Waters).

115 *Metabolic Cages*–Indirect calorimetry and activity measurements were performed with
116 Comprehensive Lab Animal Monitoring system (CLAMS) opencircuit Oxymax system (Columbus
117 Instruments). Mice were individually housed in cages with a known O_2 concentration and flow rate. After
118 one day of acclimation, measurements were carried on for four days.

119 *Bomb calorimetry*–Feces were collected from mice caged individually for a 24-hour period either
120 during ad libitum feeding or during 24-hour refeeding after a 16-hour fast. Samples were ground to a fine
121 powder and calorie content of each sample was determined with a calorimeter (Parr Instrument
122 Company).

123 *Triolein gavage*–For lipid absorption analysis the mice underwent a 4h fast between 7:00 and 11:00,
124 then were injected intraperitoneally with Poloxamer 407 (1 g/kg body weight, BASA Corp.) in PBS (29),
125 before receiving an oral gavage with 200 µl of olive oil containing 2.5 µCi of [^{3}H] triolein ([9-10-
126 ^{3}H(N)]triolein; Perkin Elmer).

127 Mice were bled before the gavage as time 0, and then at 1, 2, 4, 8, 24h post-gavage. Plasma samples
128 were analyzed for radioactivity (Tricarb 2910TR Scintillation counter; Perkin Elmer). Lipid extraction
129 from intestine was performed as described (1). For TCA treatment, mice were orally gavaged with 17
130 mg/kg taurocholic acid in 1.5% $NaHCO_3$ for three consecutive days at 6:00 pm (20), the experiment was
131 performed on the fourth day. This dose was chosen based on earlier publications demonstrating that a
132 dose in this range has limited or no effects on the BA pool of wild-type mice, but can be expected to raise
133 the TCA levels in the TCA-deficient Cyp8b1 knockout mice (19, 22).

134 *TLC separation of lipids*–Lipid extracted from the feces or jejunum of mice gavaged with [^{3}H] triolein
135 were spotted on a silica plate for thin layer chromatography (Millipore), these were developed with a
136 solvent mixture: hexane, diethyl ether, acetic acid (70/30/1 v/v). The lipid species were identified using a
137 running standard composed of the following lipids: Oleic acid, 1-Oleoyl-rac-glycerol, 1,2-Dioleoyl-sn-

glycerol, 1,3-Diolein, Triolein (all from Sigma Aldrich). Lipid species were visualized with iodine staining and corresponding spots were scraped in a scintillation tube for following radioactive counting.

Analysis of Lipids Using High Performance Liquid Chromatography-Mass Spectrometry–Lipid extracted from intestine and feces were measured separately on two platforms. Free fatty acids were measured at the Biomarkers Core Laboratory of Columbia University on a Waters Xevo TQ MS ACQUITY UPLC system (Waters, Milford, MA) as previously described (9). Other lipid species were analyzed using a 6490 Triple Quadrupole LC/MS system (Agilent Technologies, Santa Clara, CA). Glycerophospholipids and sphingolipids were separated with normal-phase HPLC as reported before (7), with a few modifications. An Agilent Zorbax Rx-Sil column (inner diameter 2.1 x 100 mm) was used under the following conditions: mobile phase A (chloroform:methanol:1 M ammonium hydroxide, 89.9:10:0.1, v/v) and mobile phase B (chloroform:methanol:water:ammonium hydroxide, 55:39.9:5:0.1, v/v); 95% A for 2 min, linear gradient to 30% A over 18 min and held for 3 min, and linear gradient to 95% A over 2 min and held for 6 min. Sterols and glycerolipids were separated with reverse-phase HPLC using an isocratic mobile phase as before (7) except with an Agilent Zorbax Eclipse XDB-C18 column (4.6 x 100 mm). Quantification of lipid species was accomplished using multiple reaction monitoring (MRM) transitions and instrument settings that were developed in earlier studies (7, 12) Each sample was spiked with a mix of internal standards, containing known concentrations for each of the following species: PA 14:0/14:0, PC 14:0/14:0, PE 14:0/14:0, PI 12:0/13:0, PS 14:0/14:0, SM d18:1/12:0, MG 17:0, 4ME 16:0 diether DG, D_5-TG 16:0/18:0/16:0 (Avanti Polar Lipids, Alabaster, AL). Endogenous lipid species levels were calculated by measuring its signal intensity relative to the signal intensity of the relevant internal standard species and multiplied by the concentration of the internal standard species.

Statistical Analyses–Data are presented as mean ± SEM. Data were analyzed by one and two-way ANOVA or student's t-tests, as reported in figure legends.

164

RESULTS

Cyp8b1$^{-/-}$ ablation eliminates 12α-hydroxy BA production and increases total BA production.–We confirmed in our independently generated, C57BL/6-backcrossed *Cyp8b1$^{-/-}$* mouse line that expression levels of *Cyp8b1* mRNA were undetectable in knockouts, while heterozygous mice had an intermediate reduction (Fig. 1A). Mice lacking Cyp8b1 have previously been shown to lack all 12α-hydroxylated BAs, while total BAs are not reduced, due to compensatory increases in non-12α-hydroxylated BAs (26). To investigate this in our mouse line, and test the gene-dosage effects, we measured the total BA pool (liver + gallbladder + small intestine) in each genotype. Complete BA data sets are provided in Table 1. We found that Cyp8b1$^{-/-}$ mice had extremely low levels of 12α-hydroxylated BAs and an expansion of the non-12α-hydroxylated BAs (Fig. 1B-C), as expected. This led to a substantial reduction in the ratio of 12α-hydroxylated to non-12α-hydroxylated BAs (Fig. 1D). There was no significant difference in BA pool size between knockouts and controls, although there was a decrease in the knockouts compared to the heterozygous mice (Fig. 1B). The heterozygous mice showed an intermediate change in BA pool composition (Fig. 1B-D). These findings demonstrate that deletion of Cyp8b1 leads to gene dosage-dependent decreases in 12α-hydroxy BA composition.

Cyp8b1$^{-/-}$ mice gain less weight when fed a western type diet–We analyzed the body weight of mice fed a standard chow diet, and at 8 weeks of age *Cyp8b1$^{-/-}$* mice had a lower body weight than littermate controls (Fig. 2A), similar to what was previously reported (20). Next we selected mice from each genotype that were weight-matched, due to natural variation, and fed them for four weeks with western type diet (WTD), containing 42% kcal from milkfat and 0.2% cholesterol. We found that *Cyp8b1$^{-/-}$* mice gained less weight than controls, leading to 15.2% lower body weight after four weeks (Fig. 2B). Analysis of body composition revealed that this difference was entirely due to fat mass, as *Cyp8b1$^{-/-}$* mice gained 47% less fat mass than controls (Fig. 2C-D). There were no differences in body length (Control: 9.50 ± 0.08 cm; *Cyp8b1$^{+/-}$* 9.41 ± 0.05 cm; *Cyp8b1$^{-/-}$* 9.31 ± 0.03 cm, p = 0.4 and 0.07). *Cyp8b1* heterozygous mice showed no significant differences in body weight or body composition compared to wild-type controls.

Consistent with their low body weight and with previously published findings (4, 20), WTD-fed Cyp8b1-deficient mice showed improved insulin sensitivity. Both *Cyp8b1*$^{-/-}$ and *Cyp8b1*$^{+/-}$ mice showed lower insulin levels after a 6–hour fast, with normal plasma glucose (Fig. 2E-F). The knockouts tended to have increased liver glycogen upon refeeding (p=0.052, Fig. 2G). These mice also showed improved oral glucose tolerance, with a 20% decreased area under the curve, compared to wild-type controls (Fig. 2H-I). These findings demonstrate that WTD-fed *Cyp8b1*$^{-/-}$ mice have improved insulin sensitivity compared to WTD-fed littermate controls. Heterozygous *Cyp8b1*$^{+/-}$ mice showed no significant difference in liver glycogen or glucose tolerance compared to controls, although their fasting insulin was lower, thus their improvements in insulin sensitivity were milder than total knockouts.

Cyp8b1$^{-/-}$ *mice are resistant to liver lipid accumulation*–There was an 80% reduction in liver acylglycerols and cholesterol of *Cyp8b1* deficient mice fed a WTD compared to littermate controls (Fig. 3A-C). *Cyp8b1*$^{-/-}$ mice showed a trend towards decreased plasma cholesterol in re-fed conditions (p=0.078), but no changes in plasma triglycerides (Fig. 3D-E). These findings demonstrate that the absence of *Cyp8b1* protects almost completely against WTD-induced hepatic steatosis.

Fecal caloric content, but not energy expenditure, can contribute to protection from western type diet feeding–Next we measured energy expenditure and metabolic fuel selection in WTD-fed mice to identify any imbalances in energy metabolism. We found no differences in energy expenditure, respiratory exchange ratio, oxygen consumption, locomotor activity, or food intake between the genotypes (Fig. 4A-E). Thus, neither excess energy expenditure nor decreased food intake can explain the low body weight of WTD-fed *Cyp8b1* knockout mice. To exclude the possibility that the difference in body weight could influence energy expenditure calculations, we also normalized the measurement per gram of body weight, but still found no differences between the genotypes (Fig. 4F).

We hypothesized that reduced intestinal lipid absorption due to the altered BA composition might explain the protection from both the body weight gain and liver lipid accumulation in *Cyp8b1*$^{-/-}$ mice. We first investigated this by performing bomb calorimetry to analyze the calorie content of the feces. We found that during both standard chow and WTD feeding, *Cyp8b1*$^{-/-}$ mice had increased fecal calorie

excretion, with a greater discrepancy with the latter diet (Fig. 5A-B), while still producing the same amount of feces (Fig. 5-C-D).

Cyp8b1 deficiency increases excretion of hydrolyzed fats–We expected that the increased calories in feces of *Cyp8b1*$^{-/-}$ mice were caused by lipid excretion. Indeed, these mice are known to have poor cholesterol absorption (30), however, the mechanisms responsible for the absorption of cholesterol and triglyceride are distinct (18). For example, bile acid composition regulates cholesterol absorption through effects on solubility of cholesterol in the lumen as well as esterification of cholesterol within the enterocyte (44). To test the absorption of dietary fat, and to determine the types of lipids excreted, we performed lipidomic analysis of fecal samples, collected over a 24-hour period. We also analyzed intestinal samples, collected after a 5-hour refeeding period. Intestinal samples contained intact tissue as well as any lumenal contents. When expressed as relative values (*Cyp8b1*$^{-/-}$ versus controls), we found that acylglycerols, and free fatty acids were substantially higher in feces of *Cyp8b1*$^{-/-}$ mice, particularly for fatty acids with longer acyl chain lengths (Fig. 6A-B, Tables 2-3). In the upper small intestine, most lipid species were normal or slightly elevated in *Cyp8b1*$^{-/-}$ mice. In the lower small intestine and large intestine *Cyp8b1*$^{-/-}$ mice had marked decreases in most lipids in these mice, except free fatty acids which were higher, especially saturated fatty acids.

When expressed quantitatively, we found that free fatty acids were the most abundant lipids in feces of *Cyp8b1*$^{-/-}$ mice, at a total concentration of 219 nmol/mg (Fig. 6C), followed by monoacylglycerols at 9.62 nmol/mg (Fig. 6D). Triglycerides, while tending to be relatively higher in *Cyp8b1*$^{-/-}$ feces compared to controls, were present at low concentrations. This indicates that the excess fat excreted by *Cyp8b1*$^{-/-}$ mice are primarily hydrolyzed triglycerides.

Intestinal lipid absorption is reduced in mice lacking Cyp8b1–In order to directly test the absorption of intestinal triglycerides, we used a radiolabeled triglyceride tracer. We injected mice with P-407 to block lipoprotein clearance (29), and administered olive oil containing [^{3}H]-triolein by oral gavage. For each genotype, we used untreated mice and those treated for three days with taurocholic acid (TCA), the major 12α-hydroxylated BA species absent from *Cyp8b1*$^{-/-}$ mice (Table 1, Fig. 1B) (26). We found that plasma

[^{3}H] levels of untreated mice reached a level 43.1% lower in *Cyp8b1*$^{-/-}$ compared to controls (Fig. 7A). However, plasma tracer levels were fully restored in mice treated with TCA, indicating that this BA species is sufficient to promote triglyceride absorption.

To determine the fate of the tracer, we measured its levels in the intestine, the lumenal contents of the colon, and in the feces. 24-hours after delivering the tracer, we found no differences between genotypes in the [^{3}H] content in the intestine (Fig. 8A). However, *Cyp8b1*$^{-/-}$ mice tended to have higher levels of the tracer in colon contents (p=0.06) and feces (p=0.16), which were normalized after TCA treatment (Fig. 7B).

We also analyzed the total acylglycerol content in these same tissues and feces. We found that in *Cyp8b1*$^{-/-}$ mice, acylglycerols tended to be decreased in the small intestine (Fig. 8B), but increased in stool, and this was normalized after TCA treatment (Fig. 7C).

To assess the hydrolysis of the triglyceride tracer, we separated lipid species from fecal lipid extracts using thin layer chromatography. Feces from *Cyp8b1*$^{-/-}$ mice tended to have increases in all lipid species, but the vast majority of tracer was found in the free fatty acid fraction (Fig. 7D). This indicates that the altered BA composition in these mice causes defective lipid absorption, but sustains normal triglyceride hydrolysis. To assess the re-esterification of the absorbed lipids within the enterocytes, we performed thin layer chromatography on jejunal tissue (Fig. 8C). We found no differences in the ratio of triglyceride to monoacylglycerol or the ratio of triglyceride to free fatty acid (Fig. 8D). This indicates that the altered BA composition in these mice does not adversely impact triglyceride synthesis in enterocytes.

Fat-free diet feeding normalizes body weight and steatosis phenotypes–To determine whether the dampened absorption of dietary fat was responsible for the differences between genotypes, we fed the mice with a fat-free diet (FFD). We performed this experiment in mice that were weight-matched, due to natural variation. In opposition to what we witnessed for normal chow and WTD, no differences in body weight developed between the two genotypes over the 4-week FFD feeding period (Fig. 9A). Moreover, FFD-fed mice showed no differences between genotypes in fat mass, liver fat, fecal acylglycerols, or fecal calories (Fig. 9B-E).

We also performed this experiment in typical cohorts where *Cyp8b1*$^{-/-}$ mice weigh less than controls at baseline, and then fed the mice the FFD. In this experiment, there was no further divergence in body weight between genotypes, and the mice gained an equal amount of fat over 4-week FFD feeding period (Fig. 9F-G). Overall, these findings demonstrate that dietary fat is the primary cause of the lean phenotype of *Cyp8b1* deficient mice.

DISCUSSION

In this work we show that CYP8B1 is necessary to promote dietary lipid absorption in mice. The absence of *Cyp8b1* led to reductions in WTD-induced weight gain, improved insulin sensitivity, and remarkable resistance to fatty liver. These changes were due to malabsorption of dietary fat, subsequent to altered BA composition, without any depletion of the total BA pool size. Amid the robust interest in the metabolic effects of BA signaling pathways, these findings reemphasize the importance of the surfactant function of these molecules in regulating systemic energy metabolism.

Cholic acid (CA), the major product of CYP8B1 activity, has been studied at length for its importance in cholesterol homeostasis. In mice, it is required for activating FXR and the downstream negative feedback loops that regulate the conversion of cholesterol into BA (26). CA also has a central role in promoting intestinal cholesterol absorption (30), an effect that is independent of FXR (32). This combination of increased cholesterol catabolism and decreased cholesterol absorption leads to reduced atherosclerosis and reduced gallstone formation in *Cyp8b1* deficient mice (32) (39, 42). Thus eliminating CA may be cardioprotective.

On the other hand, the links between 12α-hydroxylated BAs and energy metabolism have only recently been appreciated. Our lab demonstrated that human subjects in the lowest quartile of BA 12α-hydroxylation had improvements in insulin-stimulated glucose disposal as well as lower free fatty acids, triglycerides, and fatty liver (13). Thus understanding the direct links between 12α-hydroxy BAs and lipid homeostasis is relevant to humans. Recent work from two laboratories has demonstrated that *Cyp8b1*$^{-/-}$ mice have low body weight, improved glucose tolerance, and higher calorie excretion (4, 20).

In the present work we demonstrate that these changes are due to reduced absorption of dietary triglycerides, despite normal triglyceride hydrolysis and normal triglyceride synthesis in the intestinal wall. We showed that the absorption can be restored with TCA treatment. Finally, we definitively demonstrated that the effects of Cyp8b1 on body weight are due to intestinal fat, as there are no changes in energy expenditure, and the phenotypes are normalized when mice were fed a fat-free diet. These findings suggest the possibility of treating obesity by altering the bile acid pool composition to decrease 12α-hydroxy BAs (such as TCA). Such a treatment strategy may require substantial alterations in BA composition in order to affect whole body energy metabolism, as indicated by the mild phenotype of *Cyp8b1* heterozygous mice. Nevertheless, it may have the dual effect of reducing intestinal fat absorption and at the same time improving glucose metabolism.

A key mechanism by which BAs promote lipid absorption is by solubilizing lipids near the brush border membrane, to allow uptake into enterocytes. But BAs are also important for the activity of pancreatic lipase, particularly in acidic conditions, as found in the duodenum and jejunum (5). Our findings demonstrate that the altered BA composition of *Cyp8b1*$^{-/-}$ mice affects the ultimate uptake of fat into the enterocytes, despite relatively normal fat hydrolysis. Although there are some limitations in our methods– collecting feces over 24h may introduce some bias due to metabolism by fecal microbiota, and our intestinal samples are a combination of lumenal contents as well as intestinal tissue–overall these findings suggest that the physicochemical properties of BAs affect fat uptake and fat hydrolysis differently.

A wealth of prior evidence demonstrates the importance of intestinal fat absorption in body weight maintenance. A critical step in fat absorption is the glycerol phosphate pathway, where free fatty acids and monoacylglycerols absorbed by the enterocytes are re-esterified into triglycerides to be packaged into chylomicrons. This process is carried out by monoacylglycerol– and diacylglycerol acyltransferases (MGATs and DGATs). Indeed, deletion or inhibition of MGAT2 or DGAT1 results in reduced fat absorption, resistance to obesity, improved glucose tolerance, and reduced fatty liver (1, 35, 38, 45). Inhibitors of pancreatic lipase also reduce intestinal fat absorption and cause weight loss, due to excretion

of intact dietary triglycerides (17, 23). Our current finding that *Cyp8b1*$^{-/-}$ mice excrete hydrolyzed fats, and show no aberrant accumulation of lipid in the intestinal wall, indicates that the mechanisms and consequences of the lipid malabsorption in these mice are unique in comparison to inhibition of MGAT, DGAT, or pancreatic lipase.

These new data may shed light on whether aberrant regulation of *Cyp8b1* can contribute to the pathogenesis of obesity and insulin resistance. *Cyp8b1* expression is regulated by insulin action: its expression requires FOXO transcription factors, which are inactivated by insulin signaling. This is clearly shown in mice lacking *FoxO1*, which are insulin sensitive and have low levels of 12α-hydroxy BAs (15). On the other hand, murine models of diabetes have increased 12α-hydroxy BAs: genetic ablation of hepatic insulin receptor causes an increase in FOXO1 activity and a higher abundance of CA (3). A similar result was found in non-obese spontaneously diabetic (NOD) mice (36), and Alloxan-treated mice (2). This effect also occurs in human subjects with obesity and type 2 diabetes, who have higher 12α-hydroxy BA synthesis (6, 14). Our findings suggest that this change in BA pool composition may not only increase the absorption of cholesterol (2), but also dietary triglycerides. Thus it's possible that the effect of insulin resistance to change BA composition in the natural history of type 2 diabetes further worsens metabolic outcomes in a feed-forward fashion.

We have demonstrated that eliminating 12α-hydroxy BAs improves body weight, liver steatosis and lipid homeostasis during western diet feeding. This is due to reduced intestinal absorption of fat. This is of no particular hindrance in normal feeding conditions, but is protective when consuming a fat-rich diet. These findings suggest the possibility of CYP8B1 as a therapeutic target for obesity, fatty liver and hypertriglyceridemia.

Acknowledgements–We gratefully acknowledge Thomas Kolar and Ana Flete for technical assistance and Mark Erion, David Kelley, Martin Brenner, Rudy Leibel, Henry Ginsberg, Domenico Accili, Utpal Pajvani, Sei Higuchi, Santhosh Satapati, Qing Dallas-Yang and Xiaodong Yang for helpful advice and support.

Grant Support–This work was supported by funds from the NIH including R00HL111206, P30DK63068, the Hormone and Metabolite Core Facility (P30DK026687), the Biomarkers Core Facility (UL1TR001873), unrestricted funds from Merck Research Laboratories, the New York Community Trust (P14-000886), and the Russell Berrie Foundation.

Disclosure–K.K.J., L.W., and J.C.-P. are former employees of Merck Research Laboratories. G.D.P is an employee at Denali Therapeutics Inc. All other authors have no conflicts of interest to declare.

Author Contributions–E.B. designed and performed experiments, analyzed data, and wrote the manuscript. R.A.H. designed experiments, analyzed data, and wrote the manuscript. Y.X., G.D. and R.B.C performed the lipidomic studies and edited the manuscript. K.K.J., J.C.P., and L.W. supplied the *Cyp8b1* deficient mice, contributed to discussions, and edited the manuscript.

Footnotes–The content is solely the responsibility of the authors and does not necessarily represent the official views of the National Institutes of Health.

Abbreviations used in this paper–7-HCO, 7-hydroxy-4-cholesten-3-one; 7,12-diHCO, 7,12-dihydroxy-4-cholesten-3-one; αMCA, alpha-muricholic acid; βMCA, beta-muricholic acid; BA, bile acid; CA, cholic acid; CDCA, chenodeoxycholic acid; CE, cholesterol esters; DCA, deoxycholic acid; DG, diacylglycerol; FC, free cholesterol; FFD, fat free diet; GCA, glycocholic acid; GCDCA, glycochenodeoxycholic acid; GDCA, glycodeoxycholic acid; GUDCA, glycoursodeoxycholic acid; HDCA, hyodeoxycholic acid; LCA, lithocholic acid; LI, large intestine; MG, monoacylglycerol; MCA, muricholic acid; PC, phosphatidylcholine; NOD, non-obese spontaneously diabetic mice; PE, phosphatidylethanolamine; RER, respiratory exchange ratio; SI, small intestine; SM sphingomyelin; T-α & β MCA, tauro-alpha and beta muricholic acid; TCA, taurocholic acid; TCDCA taurochenodeoxycholic

371 acid; TDCA, taurodeoxycholic acid; TG, triacylglycerol; TLCA, taurolithocholic acid; UDCA,
372 ursodeoxycholic acid; WTD, western-type diet.
373
374

REFERENCES

1. **Ables GP, Yang KJ, Vogel S, Hernandez-Ono A, Yu S, Yuen JJ, Birtles S, Buckett LK, Turnbull AV, Goldberg IJ, Blaner WS, Huang LS, and Ginsberg HN.** Intestinal DGAT1 deficiency reduces postprandial triglyceride and retinyl ester excursions by inhibiting chylomicron secretion and delaying gastric emptying. *Journal of lipid research* 53: 2364-2379, 2012.
2. **Akiyoshi T, Uchida K, Takase H, Nomura Y, and Takeuchi N.** Cholesterol gallstones in alloxan-diabetic mice. *J Lipid Res* 27: 915-924, 1986.
3. **Biddinger SB, Haas JT, Yu BB, Bezy O, Jing E, Zhang W, Unterman TG, Carey MC, and Kahn CR.** Hepatic insulin resistance directly promotes formation of cholesterol gallstones. *Nature medicine* 14: 778-782, 2008.
4. **Bonde Y, Eggertsen G, and Rudling M.** Mice Abundant in Muricholic Bile Acids Show Resistance to Dietary Induced Steatosis, Weight Gain, and to Impaired Glucose Metabolism. *PloS one* 11: e0147772, 2016.
5. **Borgström B.** Influence of bile salt, pH, and time on the action of pancreatic lipase; physiological implications. *J Lipid Res* 5: 522-531, 1964.
6. **Brufau G, Stellaard F, Prado K, Bloks VW, Jonkers E, Boverhof R, Kuipers F, and Murphy EJ.** Improved glycemic control with colesevelam treatment in patients with type 2 diabetes is not directly associated with changes in bile acid metabolism. *Hepatology* 52: 1455-1464, 2010.
7. **Chan RB, Oliveira TG, Cortes EP, Honig LS, Duff KE, Small SA, Wenk MR, Shui G, and Di Paolo G.** Comparative lipidomic analysis of mouse and human brain with Alzheimer disease. *The Journal of biological chemistry* 287: 2678-2688, 2012.
8. **Chiang JY.** Bile acids: regulation of synthesis. *Journal of lipid research* 50: 1955-1966, 2009.
9. **Clugston RD, Jiang H, Lee MX, Piantedosi R, Yuen JJ, Ramakrishnan R, Lewis MJ, Gottesman ME, Huang LS, Goldberg IJ, Berk PD, and Blaner WS.** Altered hepatic lipid metabolism in C57BL/6 mice fed alcohol: a targeted lipidomic and gene expression study. *Journal of lipid research* 52: 2021-2031, 2011.
10. **de Aguiar Vallim TQ, Tarling EJ, and Edwards PA.** Pleiotropic roles of bile acids in metabolism. *Cell metabolism* 17: 657-669, 2013.
11. **Folch J, Lees M, and Sloane Stanaley GH.** A simple method for the isolation and purification of total lipides from animal tissues. 226: 497-509, 1957.
12. **Gulati S, Ekland EH, Ruggles KV, Chan RB, Jayabalasingham B, Zhou B, Mantel PY, Lee MC, Spottiswoode N, Coburn-Flynn O, Hjelmqvist D, Worgall TS, Marti M, Di Paolo G, and Fidock DA.** Profiling the Essential Nature of Lipid Metabolism in Asexual Blood and Gametocyte Stages of Plasmodium falciparum. *Cell Host Microbe* 18: 371-381, 2015.
13. **Haeusler RA, Astiarraga B, Camastra S, Accili D, and Ferranini E.** Human Insulin Resistance Is Associated With Increased Plasma Levels of 12α-Hydroxylated Bile Acids. *Diabetes* 62: 4184-4191, 2013.
14. **Haeusler RA, Camastra S, Nannipieri M, Astiarraga B, Castro-Perez J, Xie D, Wang L, Chakravarthy M, and Ferrannini E.** Increased Bile Acid Synthesis and Impaired Bile Acid Transport in Human Obesity. *The Journal of clinical endocrinology and metabolism* 101: 1935-1944, 2016.

15. **Haeusler RA, Pratt-Hyatt M, Welch CL, Klaassen CD, and Accili D.** Impaired generation of 12-hydroxylated bile acids links hepatic insulin signaling with dyslipidemia. *Cell metabolism* 15: 65-74, 2012.
16. **Halldorsdottir S, Carmody J, Boozer CN, C.A. L, and Leibel RL.** Reproducibility and accuracy of body composition assessments in mice by dual energy x-ray absorptiometry and time domain nuclear magnetic resonance. *Int J Body Compos Res* 7: 147-154, 2009.
17. **Heck AM, Yanovski JA, and Calis KA.** Orlistat, a New Lipase Inhibitor for the Management of Obesity. *Pharmacotherapy* 20: 270-279, 2000.
18. **Iqbal J and Hussain MM.** Intestinal lipid absorption. *American journal of physiology Endocrinology and metabolism* 296: E1183-1194, 2009.
19. **Jones RD, Repa JJ, Russell DW, Dietschy JM, and Turley SD.** Delineation of biochemical, molecular, and physiological changes accompanying bile acid pool size restoration in Cyp7a1(-/-) mice fed low levels of cholic acid. *American journal of physiology Gastrointestinal and liver physiology* 303: G263-274, 2012.
20. **Kaur A, Patankar JV, de Haan W, Ruddle P, Wijesekara N, Groen AK, Verchere B, Singaraja RR, and Hayden MR.** Loss of Cyp8b1 Improves Glucose Homeostasis by Increasing GLP. *Diabetes* 64: 1168-1179, 2015.
21. **Kawamata Y, Fujii R, Hosoya M, Harada M, Yoshida H, Miwa M, Fukusumi S, Habata Y, Itoh T, Shintani Y, Hinuma S, Fujisawa Y, and Fujino M.** A G protein-coupled receptor responsive to bile acids. *The Journal of biological chemistry* 278: 9435-9440, 2003.
22. **Keane MH, Overmars H, Wikander TM, Ferdinandusse S, Duran M, Wanders RJ, and Faust PL.** Bile acid treatment alters hepatic disease and bile acid transport in peroxisome-deficient PEX2 Zellweger mice. *Hepatology* 45: 982-997, 2007.
23. **Kelley DE, Bray GA, Pi-Sunyer FX, Klein S, Hill J, Miles J, and Hollander P.** Clinical Efficacy of Orlistat Therapy in Overweight and Obese Patients With Insulin-Treated Type 2 Diabetes. *Diabetes care* 25: 1033-1041, 2002.
24. **Kuipers F, Bloks VW, and Groen AK.** Beyond intestinal soap--bile acids in metabolic control. *Nature reviews Endocrinology* 10: 488-498, 2014.
25. **Lew JL, Zhao A, Yu J, Huang L, De Pedro N, Pelaez F, Wright SD, and Cui J.** The farnesoid X receptor controls gene expression in a ligand- and promoter-selective fashion. *The Journal of biological chemistry* 279: 8856-8861, 2004.
26. **Li-Hawkins J, Gåfvels M, Olin M, Lund EG, Andersson U, Schuster G, Björkhem I, Russell DW, and Eggertsen G.** Cholic acid mediates negative feedback regulation of bile acid synthesis in mice. *Journal of Clinical Investigation* 110: 1191-1200, 2002.
27. **Makishima M, Okamoto AY, Repa JJ, Tu H, Learned RM, Luk A, Hull MV, Lustig KD, Mangelsdorf DJ, and Shan B.** Identification of a nuclear receptor for bile acids. *Science* 284: 1362-1365, 1999.
28. **Maruyama T, Miyamoto Y, Nakamura T, Tamai Y, Okada H, Sugiyama E, Nakamura T, Itadani H, and Tanaka K.** Identification of membrane-type receptor for bile acids (M-BAR). *Biochem Biophys Res Commun* 298: 714-719, 2002.
29. **Millar JS, Cromley DA, McCoy MG, Rader DJ, and Billheimer JT.** Determining hepatic triglyceride production in mice: comparison of poloxamer 407 with Triton WR-1339. *Journal of lipid research* 46: 2023-2028, 2005.
30. **Murphy C, Parini P, Wang J, Bjorkhem I, Eggertsen G, and Gafvels M.** Cholic acid as key regulator of cholesterol synthesis, intestinal absorption and hepatic storage in mice. *Biochimica et biophysica acta* 1735: 167-175, 2005.

31. **Parks DJ, Blanchard SG, Bledsoe RK, Chandra G, Consler TG, Kliewer SA, Stimmel JB, Willson TM, Zavacki AM, Moore DD, and Lehmann JM.** Bile acids: natural ligands for an orphan nuclear receptor. *Science* 284: 1365-1368, 1999.
32. **Slatis K, Gafvels M, Kannisto K, Ovchinnikova O, Paulsson-Berne G, Parini P, Jiang ZY, and Eggertsen G.** Abolished synthesis of cholic acid reduces atherosclerotic development in apolipoprotein E knockout mice. *Journal of lipid research* 51: 3289-3298, 2010.
33. **Song P, Rockwell CE, Cui JY, and Klaassen CD.** Individual bile acids have differential effects on bile acid signaling in mice. *Toxicology and applied pharmacology* 283: 57-64, 2015.
34. **Thomas C, Pellicciari R, Pruzanski M, Auwerx J, and Schoonjans K.** Targeting bile-acid signalling for metabolic diseases. *Nature reviews Drug discovery* 7: 678-693, 2008.
35. **Tsuchida T, Fukuda S, Aoyama H, Taniuchi N, Ishihara T, Ohashi N, Sato H, Wakimoto K, Shiotani M, and Oku A.** MGAT2 deficiency ameliorates high-fat diet-induced obesity and insulin resistance by inhibiting intestinal fat absorption in mice. *Lipids Health Dis* 11: 75, 2012.
36. **Uchida K, Makino S, and Akiyoshi T.** Altered bile acid metabolism in nonobese, spontaneously diabetic (NOD) mice. *Diabetes* 34: 79-83, 1985.
37. **Uchida K, Satoh T, Takase H, Nomura Y, Takasu N, Kurihara H, and Takeuchi N.** Altered bile acid metabolism related to atherosclerosis in alloxan diabetic rats. *J Atheroscler Thromb* 3: 52-58, 1996.
38. **Villanueva CJ, Monetti M, Shih M, Zhou P, Watkins SM, Bhanot S, and Farese RV, Jr.** Specific role for acyl CoA:Diacylglycerol acyltransferase 1 (Dgat1) in hepatic steatosis due to exogenous fatty acids. *Hepatology* 50: 434-442, 2009.
39. **Wang DQ, Lammert F, Cohen DE, Paigen B, and Carey MC.** Cholic acid aids absorption, biliary secretion, and phase transitions of cholesterol in murine cholelithogenesis. *Am J Physiol* 276: G751-760, 1999.
40. **Wang DQH, Tazuma S, Cohen DE, and Carey MC.** Feeding natural hydrophilic bile acids inhibits intestinal cholesterol absorption studies in the gallstone-susceptible mouse. *Physiol Gastrointest Liver Physiol* 285: G494-502, 2003.
41. **Wang DY, Chen J, Hollister K, Sowers LC, and Forman BM.** Endogenous Bile Acids Are Ligands for the Nuclear Receptor FXR/BAR. *Mol Cell* 3: 543-553, 1999.
42. **Wang J, Gafvels M, Rudling M, Murphy C, Bjorkhem I, Einarsson C, and Eggertsen G.** Critical role of cholic acid for development of hypercholesterolemia and gallstones in diabetic mice. *Biochemical and biophysical research communications* 342: 1382-1388, 2006.
43. **Watt S and Simmonds W.** Effects of four taurine-conjugated bile acids on mucosal uptake and lymphatic absorption of cholesterol in the rat. *J Lipid Res* 25: 448-455, 1984.
44. **Watt SM and Simmonds WJ.** The specificity of bile salts in the intestinal absorption of micellar cholesterol in the rat. *Clin Exp Pharmacol Physiol* 3: 305-322, 1976.
45. **Yen CL, Cheong ML, Grueter C, Zhou P, Moriwaki J, Wong JS, Hubbard B, Marmor S, and Farese RV, Jr.** Deficiency of the intestinal enzyme acyl CoA:monoacylglycerol acyltransferase-2 protects mice from metabolic disorders induced by high-fat feeding. *Nature medicine* 15: 442-446, 2009.

FIGURE LEGENDS

Figure 1. *Cyp8b1* expression and bile acid quantitation. (A) Liver gene expression of *Cyp8b1*. (B) Absolute quantitation of the total bile acid pool. 12-hydroxylated bile acids are colored in shades of blue. Non-12-hydroxylated bile acids are colored in shades of red. (C) Relative bile acid pool composition. (D) Ratio of 12-hydroxylated to non-12-hydroxylated bile acids. *P<0.05, **P<0.01, ***P<0.001, ****P<0.0001 between indicated groups. ^{aa}P<0.01, ^{aaa}P<0.001 ^{aaaa}P<0.0001 compared to control, ^{bb}P<0.01 ^{bbbb}P<0.0001 compared to heterozygous. Symbols in blue show statistics for comparisons of 12-hydroxylated bile acids. Symbols in red show statistics for comparisons of non-12-hydroxylated bile acids. TMCA = **T-α & β MCA.**

Figure 2. Body weight, mass composition, and glucose tolerance. (A) Body weight of mice on chow diet. (B) Body weight curve on western-type diet (WTD). (C) Body mass composition at the beginning (t0) and after 4 weeks WTD feeding. (D) Change in mass due to WTD. (E-F) Plasma insulin and glucose after an overnight fast. (G) Hepatic content of glycogen after 4 hours refeeding WTD. (H-I) Oral glucose tolerance test and area under the curve. (n=7).Values are displayed as mean ± SEM. For acylglycerols and cholesterol, values were averaged from two technical replicates. Statistical significance is represented as:*p <0.05, **p <0.01 measured by one-way ANOVA. For panel B, we used ANOVA with repeated measures.

Figure 3. Hepatic and circulating lipids. (A-C) Hepatic acylglycerols and cholesterol during chow and WTD feeding, and Oil Red O staining of frozen livers. Scalebar is 200 μm. (D-E) Plasma levels of cholesterol and acylglycerols in the ad libitum fed and overnight fasted state. (n=7).Values are displayed as mean ± SEM. For cholesterol, and acylglycerols, results are averaged from two technical replicates. Statistical significance is represented as: ****p < 0.0001 *Cyp8b1*$^{+/-}$ vs control, measured by one-way ANOVA.

Figure 4. Energy expenditure and fecal caloric output. (A-D) Indirect calorimetry measurement of heat production, respiratory exchange ratio, volume of oxygen consumed and locomotor activity. (E) 24–hour food intake on WTD. (F) Quantification of heat production per gram of body weight. (n=8) Values are displayed as mean ± SEM.

Figure 5. Fecal caloric output. (A-B) Fecal caloric content from chow and WTD-fed mice, as measured by bomb calorimetry. (C-D) Fecal mass output from chow and WTD-fed mice collected over a 24h period. (n=8) Values are displayed as mean ± SEM, values were averaged from two technical replicates. Statistical significance is shown as: *p <0.05, **p <0.01, measured by two-way ANOVA.

Figure 6. Lipidomic analysis. (A-B) Heatmaps representing the ratio of *Cyp8b1*$^{-/-}$ mice to littermate controls for lipid species in intestinal tissue and feces. (A) tri- di- and monoacylglycerol [TG, DG, MG] and (B) free fatty acids. (C-D) Quantitation of lipid species in feces (n=8).

Figure 7. Lipid absorption. (A) Plasma [^{3}H]-triolein-derived counts (cpm) in untreated (left) and TCA-treated mice (right). (B) [^{3}H] counts in feces and colon contents (cpm/mg). (C) Total acylgycerols in feces and colon contents. (D) Triolein-derived [^{3}H] counts in lipid species separated by thin layer chromatography. (n=6) Statistical significance is represented as: **p <0.01, measured by one-way ANOVA.

Figure 8. Lipid accumulation in the enterocytes. (A) Triolein-derived [^{3}H] in intestinal wall (cpm/mg). (B) Total acylglycerols in intestine. (C) Triolein-derived counts in lipid species separated by thin layer chromatography in jejunum (cpm/mg). (D) Ratio of TAG to MAG and TAG to FFA. (n=6)

Figure 9. Fat free diet feeding. (A) Body weight curves of mice on fat free diet, for mice starting at the same body weight. Panels B-E show measurements from these mice. (B) Body mass composition after 3 weeks FFD feeding. (C) Hepatic levels of acylglycerols and cholesterol. (D) Levels of fecal acylglycerols. (E) Fecal caloric content from mice fed FFD, ad libitum. (F) Body weight curve of mice on FFD. (G) Fat mass gain after 4 weeks of FFD feeding, for same mice shown in panel F. (n=6) Values are displayed as mean ± SEM, statistical significance is represented as: *p <0.05, **p <0.01, *Cyp8b1*$^{-/-}$ vs control, measured by one-way ANOVA.

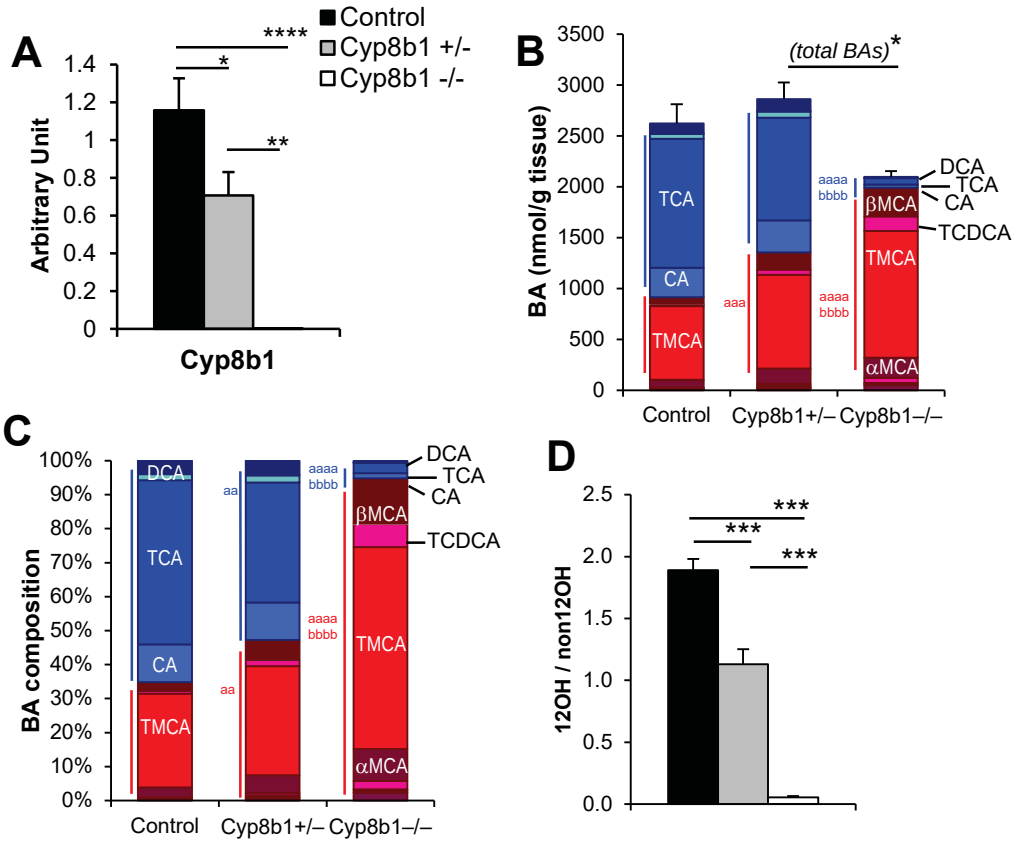
A
Control
Cyp8b1 +/-
Cyp8b1 -/-
****
*
**
Arbitrary Unit
1.4
1.2
1
0.8
0.6
0.4
0.2
0
Cyp8b1
B
(total BAs)*
BA (nmol/g tissue)
3500
3000
2500
2000
1500
1000
500
0
TCA
CA
TMCA
aaa
aaaa
bbbb
DCA
TCA
CA
βMCA
TCDCA
TMCA
αMCA
Control
Cyp8b1+/–
Cyp8b1–/–
C
BA composition
100%
90%
80%
70%
60%
50%
40%
30%
20%
10%
0%
DCA
TCA
CA
TMCA
aa
aaaa
bbbb
βMCA
TCDCA
αMCA
Control
Cyp8b1+/–
Cyp8b1–/–
D
12OH / non12OH
2.5
2.0
1.5
1.0
0.5
0.0
***
***
***

Figure 1

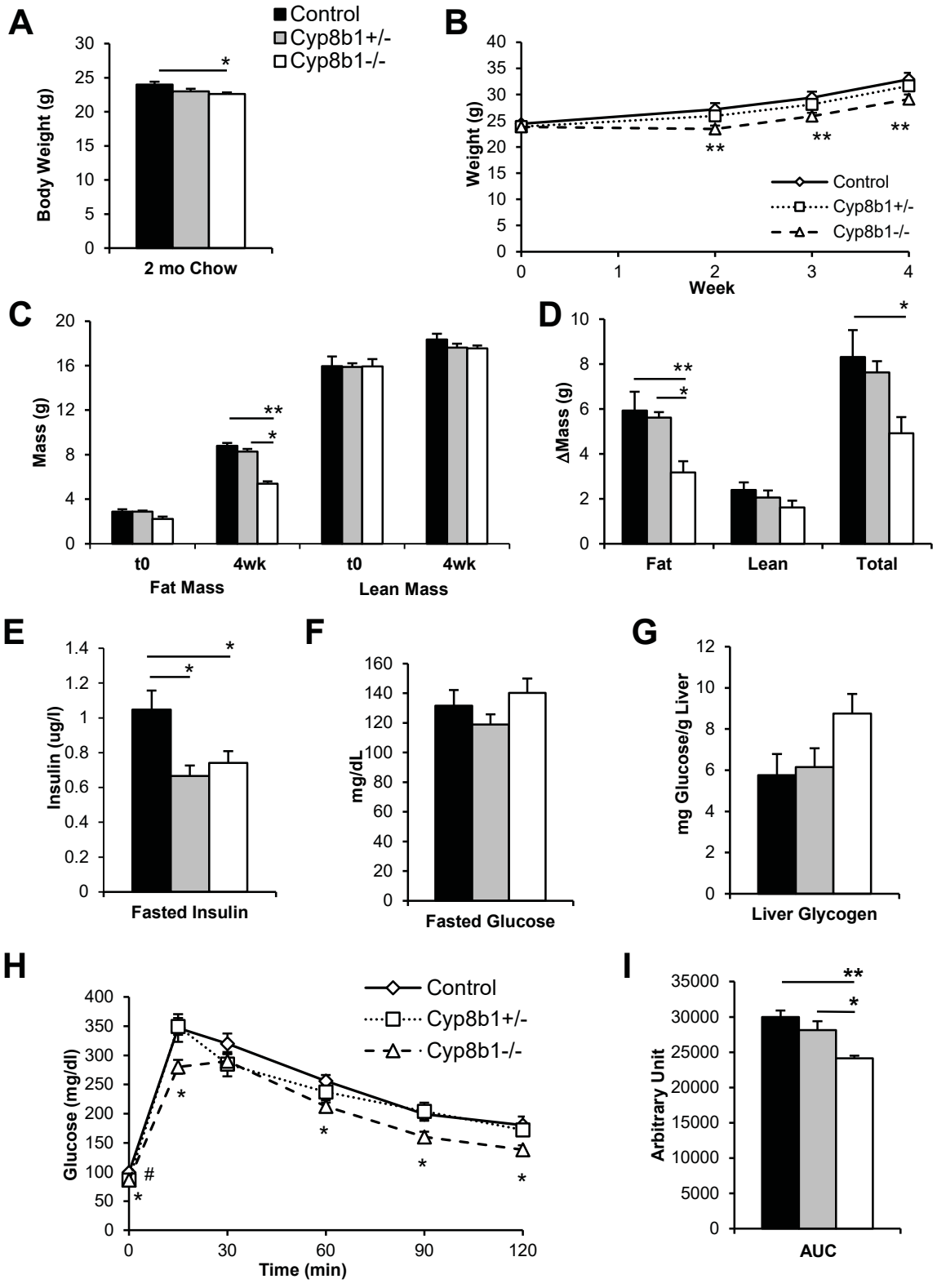
A
Control
Cyp8b1+/-
Cyp8b1-/-
Body Weight (g)
2 mo Chow
B
Weight (g)
Week
Control
Cyp8b1+/-
Cyp8b1-/-
C
Mass (g)
t0
4wk
t0
4wk
Fat Mass
Lean Mass
D
ΔMass (g)
Fat
Lean
Total
E
Insulin (ug/l)
Fasted Insulin
F
mg/dL
Fasted Glucose
G
mg Glucose/g Liver
Liver Glycogen
H
Control
Cyp8b1+/-
Cyp8b1-/-
Glucose (mg/dl)
Time (min)
I
Arbitrary Unit
AUC

Figure 2

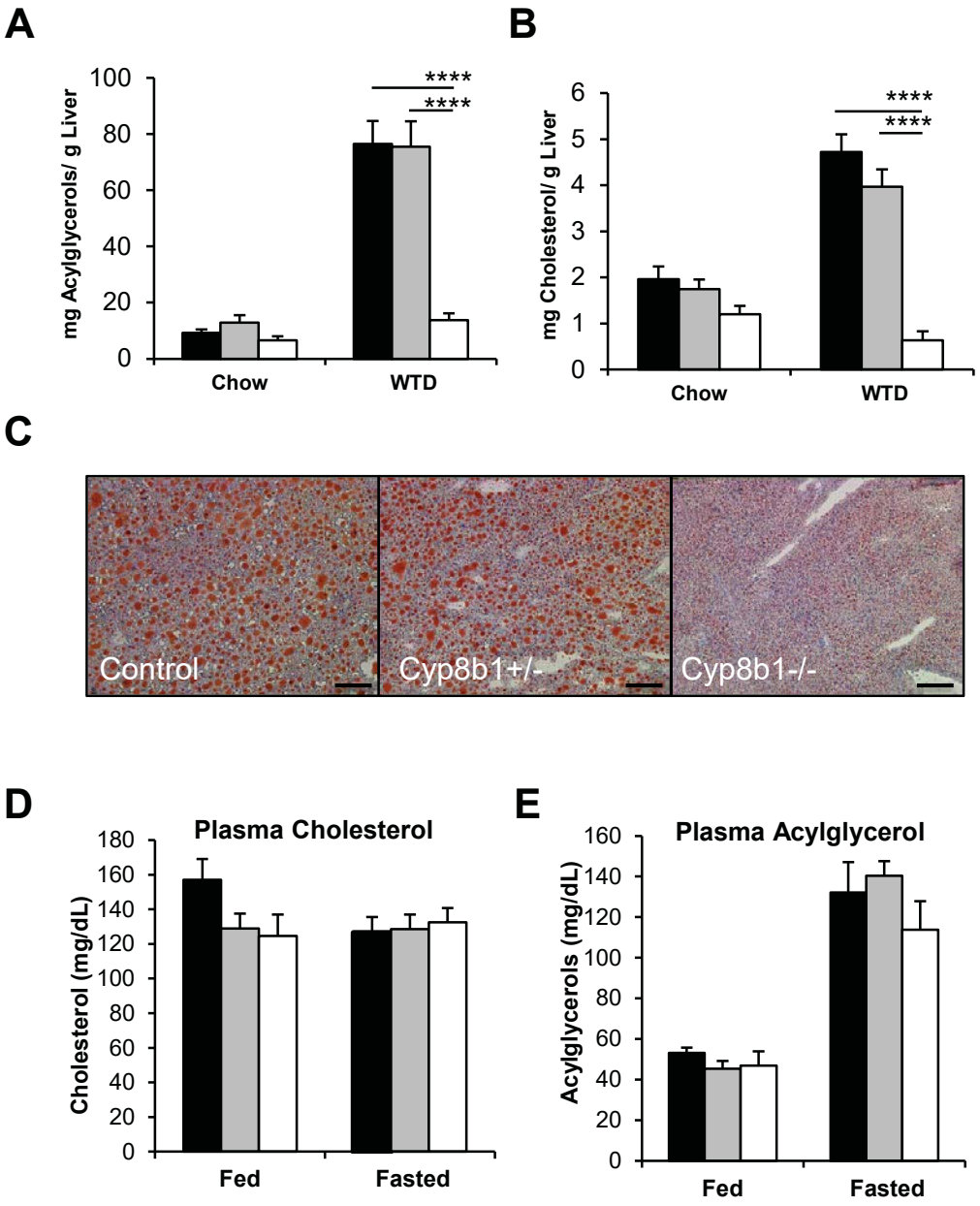
A
B
C
D
E
mg Acylglycerols/ g Liver
mg Cholesterol/ g Liver
****
****
Chow
WTD
Control
Cyp8b1+/-
Cyp8b1-/-
Plasma Cholesterol
Cholesterol (mg/dL)
Fed
Fasted
Plasma Acylglycerol
Acylglycerols (mg/dL)

Figure 3

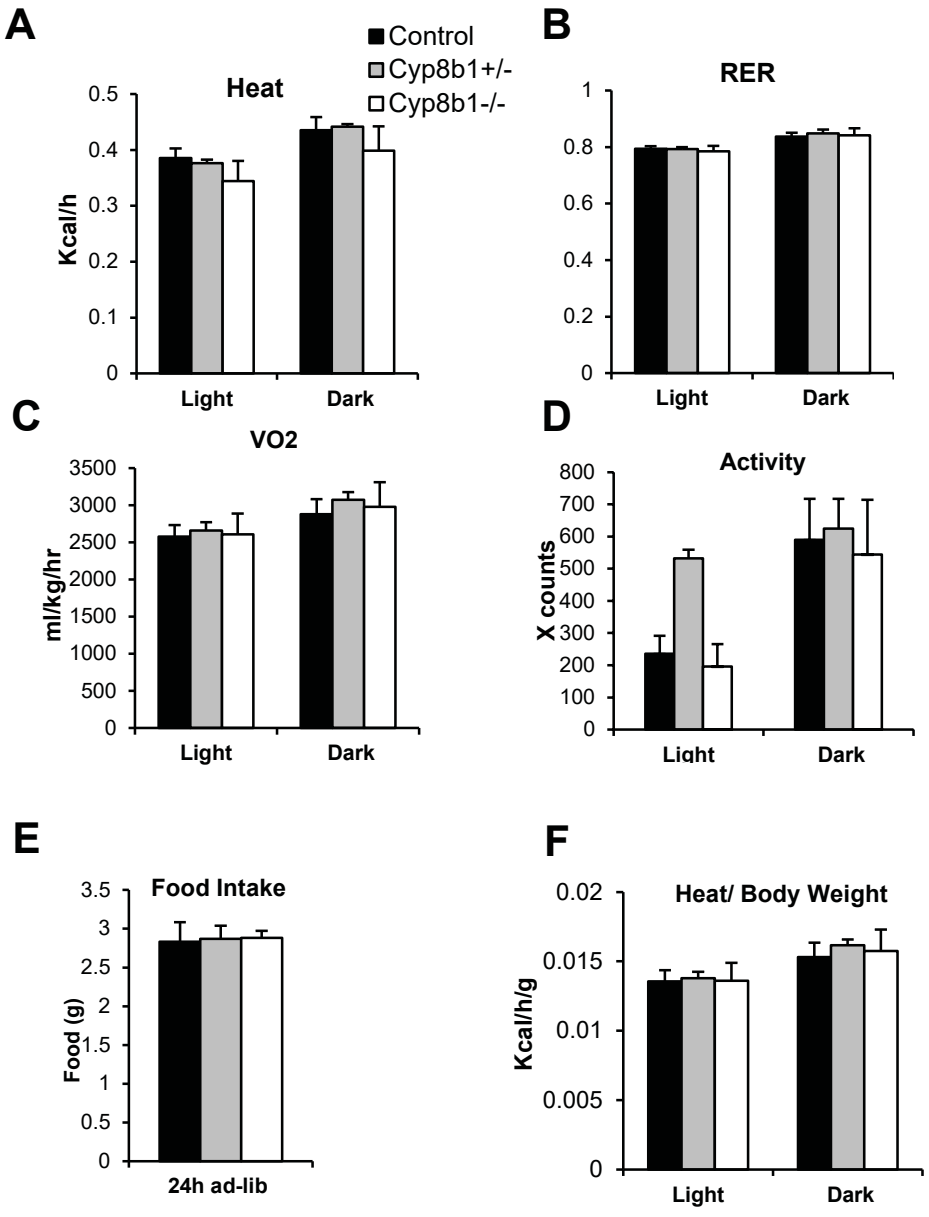
A
Control
Cyp8b1+/-
Cyp8b1-/-
Heat
Kcal/h
0.5
0.4
0.3
0.2
0.1
0
Light
Dark
B
RER
1
0.8
0.6
0.4
0.2
0
Light
Dark
C
VO2
ml/kg/hr
3500
3000
2500
2000
1500
1000
500
0
Light
Dark
D
Activity
X counts
800
700
600
500
400
300
200
100
0
Light
Dark
E
Food Intake
Food (g)
3.5
3
2.5
2
1.5
1
0.5
0
24h ad-lib
F
Heat/ Body Weight
Kcal/h/g
0.02
0.015
0.01
0.005
0
Light
Dark

Figure 4

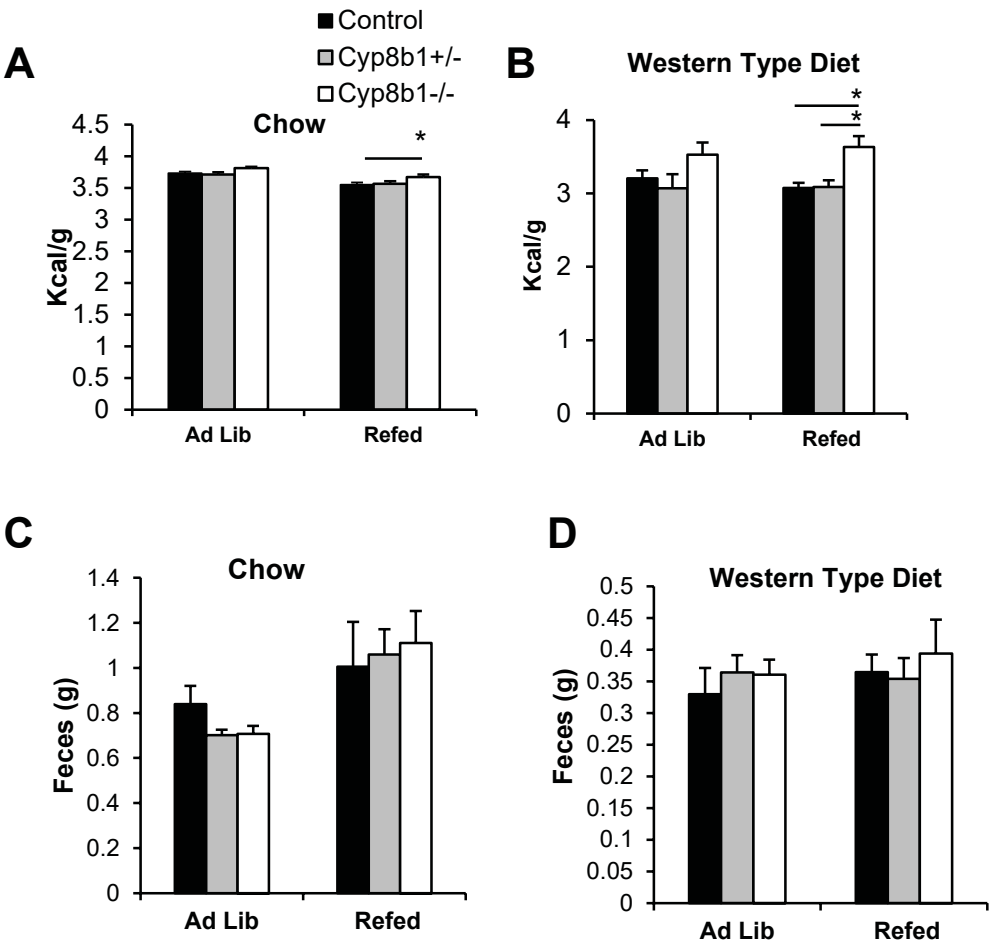
A
Control
Cyp8b1+/-
Cyp8b1-/-
Chow
Kcal/g
4.5
4
3.5
3
2.5
2
1.5
1
0.5
0
*
Ad Lib
Refed
B
Western Type Diet
Kcal/g
4
3
2
1
0
*
*
Ad Lib
Refed
C
Chow
Feces (g)
1.4
1.2
1
0.8
0.6
0.4
0.2
0
Ad Lib
Refed
D
Western Type Diet
Feces (g)
0.5
0.45
0.4
0.35
0.3
0.25
0.2
0.15
0.1
0.05
0
Ad Lib
Refed

Figure 5

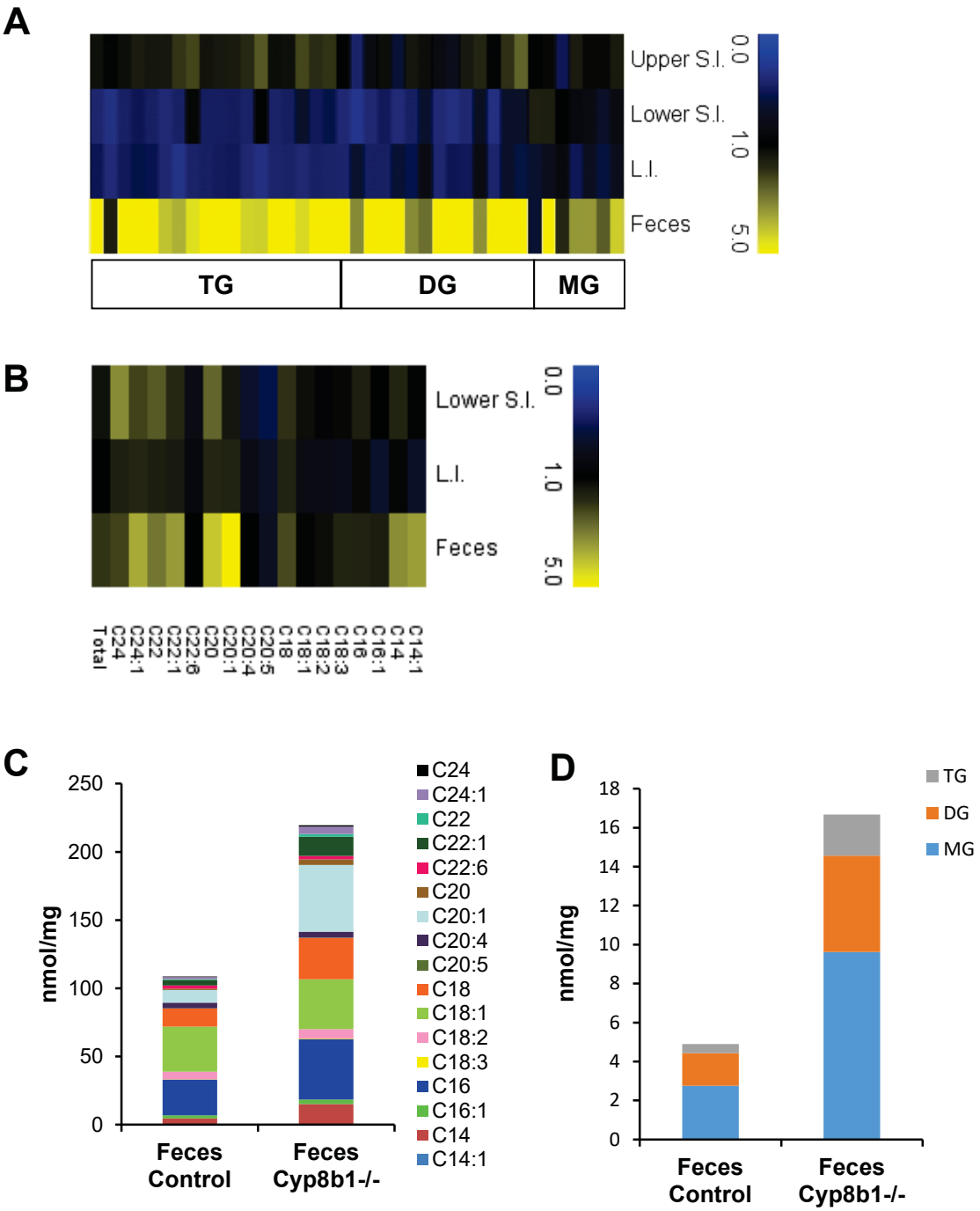
A
Upper S.I.
Lower S.I.
L.I.
Feces
0.0
1.0
5.0
TG
DG
MG
B
Lower S.I.
L.I.
Feces
0.0
1.0
5.0
Total
C24
C24:1
C22
C22:1
C22:6
C20
C20:1
C20:4
C20:5
C18
C18:1
C18:2
C18:3
C16
C16:1
C14
C14:1
C
nmol/mg
250
200
150
100
50
0
Feces Control
Feces Cyp8b1-/-
C24
C24:1
C22
C22:1
C22:6
C20
C20:1
C20:4
C20:5
C18
C18:1
C18:2
C18:3
C16
C16:1
C14
C14:1
D
nmol/mg
18
16
14
12
10
8
6
4
2
0
Feces Control
Feces Cyp8b1-/-
TG
DG
MG

Figure 6

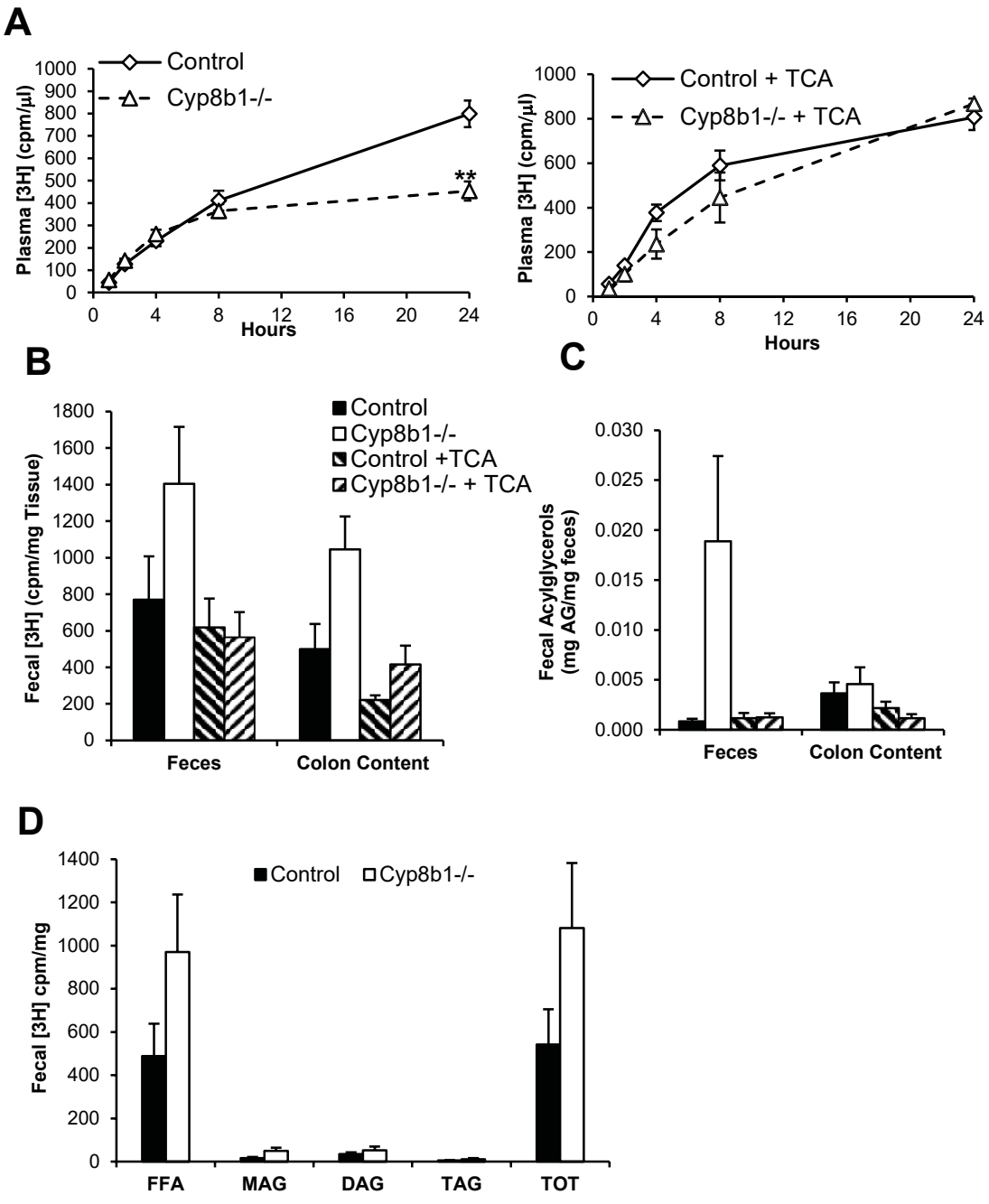
A
Control
Cyp8b1-/-
Plasma [3H] (cpm/µl)
Hours
**
Control + TCA
Cyp8b1-/- + TCA
B
Control
Cyp8b1-/-
Control +TCA
Cyp8b1-/- + TCA
Fecal [3H] (cpm/mg Tissue)
Feces
Colon Content
C
Fecal Acylglycerols (mg AG/mg feces)
D
Fecal [3H] cpm/mg
FFA
MAG
DAG
TAG
TOT

Figure 7

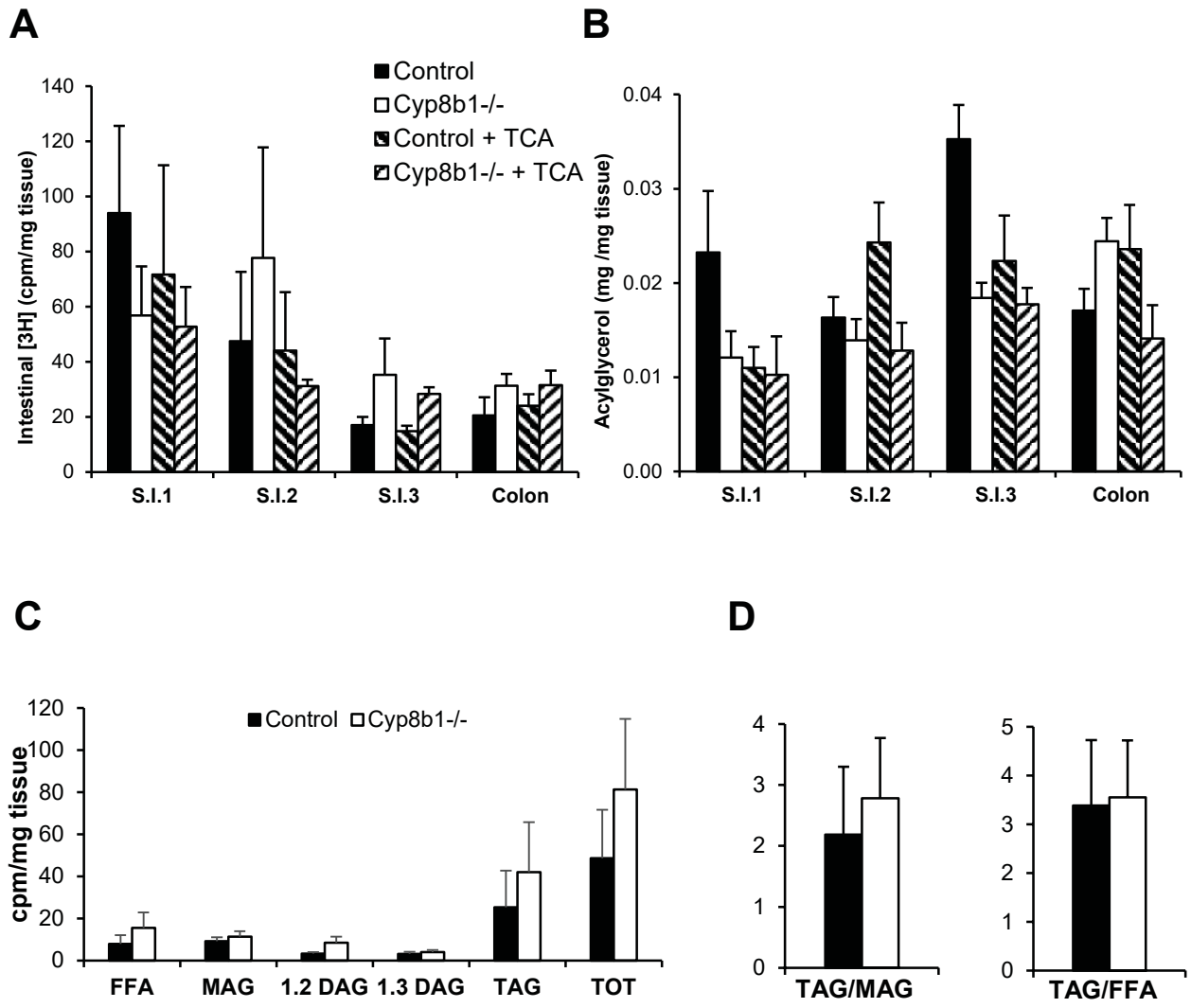
A
Control
Cyp8b1-/-
Control + TCA
Cyp8b1-/- + TCA
Intestinal [3H] (cpm/mg tissue)
140
120
100
80
60
40
20
0
S.I.1
S.I.2
S.I.3
Colon
B
Acylglycerol (mg /mg tissue)
0.04
0.03
0.02
0.01
0.00
S.I.1
S.I.2
S.I.3
Colon
C
Control
Cyp8b1-/-
cpm/mg tissue
120
100
80
60
40
20
0
FFA
MAG
1.2 DAG
1.3 DAG
TAG
TOT
D
4
3
2
1
0
TAG/MAG
5
4
3
2
1
0
TAG/FFA

Figure 8

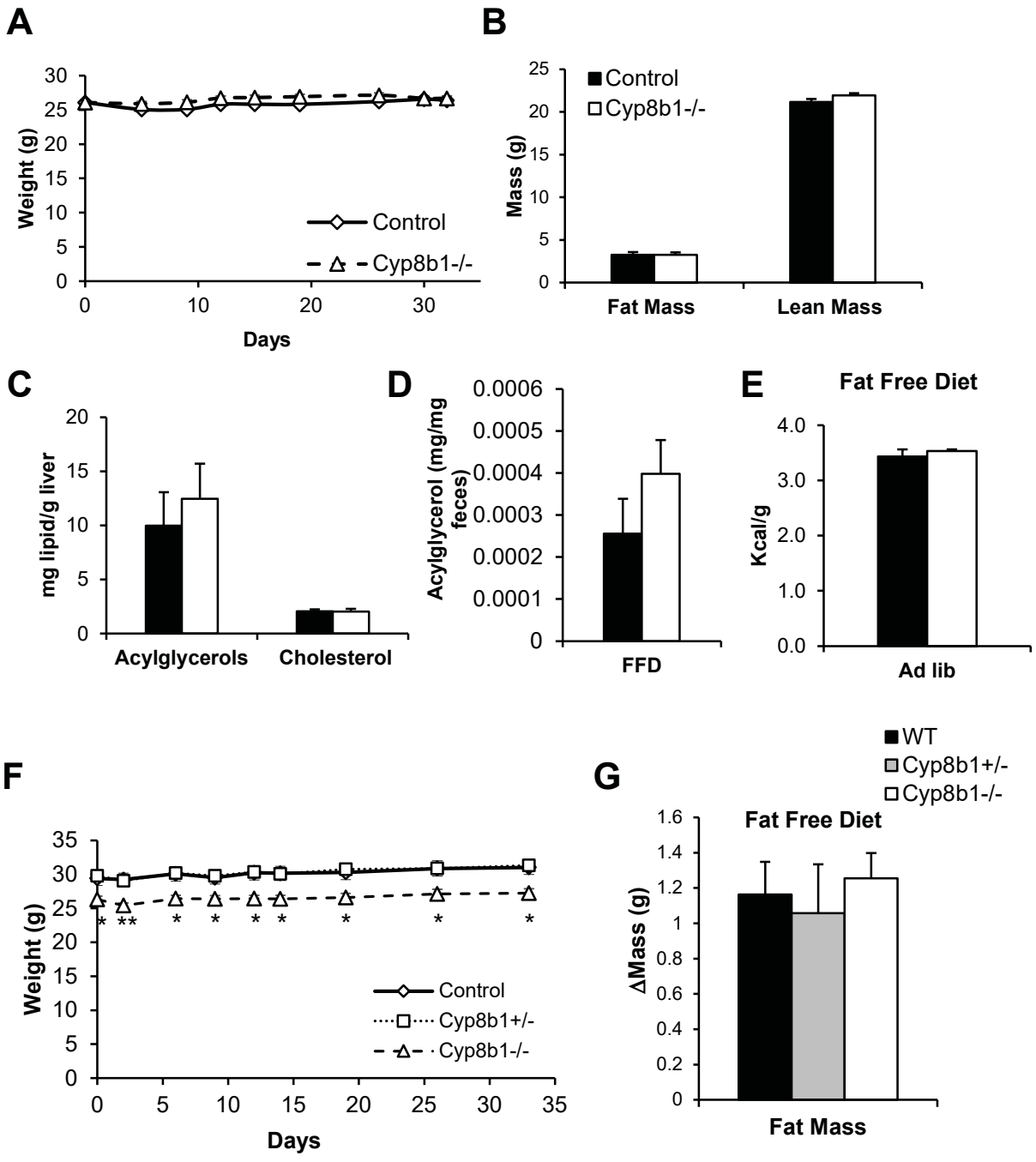
A
Weight (g)
Days
Control
Cyp8b1-/-
B
Mass (g)
Control
Cyp8b1-/-
Fat Mass
Lean Mass
C
mg lipid/g liver
Acylglycerols
Cholesterol
D
Acylglycerol (mg/mg feces)
FFD
E
Fat Free Diet
Kcal/g
Ad lib
F
Weight (g)
Days
Control
Cyp8b1+/-
Cyp8b1-/-
G
WT
Cyp8b1+/-
Cyp8b1-/-
Fat Free Diet
ΔMass (g)
Fat Mass

Figure 9

Table 1. Total levels of bile acids (nmol/g) assessed by LC-MS/MS.

	Control	Cyp8b1$^{+/-}$	Cyp8b1$^{-/-}$
CA (12-OH)	292.1 ± 45.1	314.5 ± 75.8	31.2 ± 7.8 $^{*\ \#}$
DCA (12-OH)	94.5 ± 10.9	116.6 ± 12.1	11.1 ± 2.6 $^{***\ \#\#\#\#}$
TCA (12-OH)	1267 ± 115.9	1009.8 ± 17.8	63.4 ± 20.4 $^{****\ \#\#\#}$
GCA (12-OH)	8.9 ± 0.5	7.7 ± 0.9	1.3 $^{****\ \#\#\#\#}$
TDCA (12-OH)	46.9 ±5.3	60.5 ± 11.9	2.4 ± 0.6 $^{**\ \#\#\#}$
GDCA (12-OH)	nd	nd	nd
CDCA	6.1 ± 1.1	18.33 ± 3	50.5 ± 10.2 $^{***\ \#\#}$
LCA	2.9 ± 0.3	7.0 ± 0.5	13.2 ± 3.4 $^{**\ \#}$
UDCA	8.1 ± 1.2	20.2 ± 7	48.9 ± 10.5 $^{**\ \#}$
HDCA	5.2 ± 0.8	14.9 ± 1.4 **	6.6 ± 2.4 $^{\#\#}$
TCDCA	21 ± 1.7	50.8 ± 6.2	142.8 ± 27.2 $^{****\ \#\#\#}$
GCDCA	0.2	0.3 ± 0.02	0.8 ± 0.2 $^{**\ \#\#}$
TLCA	0.4 ± 0.1	0.9 ± 0.1	1.5 ± 0.4 **
GUDCA	nd	0.6 ± 0.0	1 ± 0.1
αMCA	78.2 ± 7.4	152 ± 8.2 *	198.3 ± 41 **
βMCA	65.8 ± 13.3	168.4 ± 47.1	279.6 ± 36.8 **
T-α & βMCA	724.7 ± 64.9	920.3 ± 47.4	1246 ± 107 $^{***\ \#}$
Total	2622.7 ± 189.2	2862.8 ± 163.6	2098.9 ± 54.2 $^{\#}$
Sum 12-hydroxy	1709.5 ±124	1509 ± 155	109.5 ± 21.4 $^{****\ \#\#\#\#}$
Sum non-12-hydroxy	913.2 ± 74.3	1353.4 ± 63.5 ***	1989.4 ± 44.3 $^{****\ \#\#\#\#}$

CA, cholic acid; DCA, deoxycholic acid; TCA, taurocholic acid; GCA, glycolcholic acid; TDCA, taurodeoxycholic acid; GDCA, glycodeoxycholic acid; CDCA, chenodeoxycholic acid; LCA, lithocholic acid; UDCA, ursodeoxycholic acid; HDCA, hyodeoxycholic acid; TCDCA taurochenodeoxycholic acid; GCDCA, glycochenodeoxycholic acid; TLCA, taurolithocholic acid; GUDCA, glycoursodeoxycholic acid; αMCA, alpha-muricholic acid; βMCA, beta-muricholic acid; T-α & β MCA, tauro-alpha and beta muricholic acid. Species marked (12-OH) are 12α-hydroxylated. Those that are unmarked are non-12α-hydroxylated. Data are expressed as mean ± SEM. *p <0.05 , **p <0.01 , ***p <0.001 , ****p < 0.0001 versus Control, $^{\#}$p <0.05 , $^{\#\#}$p <0.01 , $^{\#\#\#}$p <0.001 , $^{\#\#\#\#}$p < 0.0001 versus Cyp8b1+/- measured by 1way ANOVA (n=6). nd=not detected. Sum 12-hydroxy is the sum of CA, DCA, TCA, CA

Table 2. Total levels of free fatty acids in intestine and feces (nmol/mg) assessed by HPLC-MS.

	S. I. Control	S. I. Cyp8b1-/-	L. I. Control	L. I. Cyp8b1-/-	Feces Control	Feces Cyp8b1-/-
C14	11.47 ± 1.70	19.78 ± 1.54 **	5.61 ± 0.69	6.35 ± 0.94	4.54 ± 1.82	14.92 ± 4.89
C14:1	0.29 ± 0.03	0.33 ± 0.03	0.13 ± 0.01	0.09 ± 0.01	0.05 ± 0.01	0.18 ± 0.04 **
C16	29.90 ± 2.91	47.93 ± 3.00 ***	18.35 ± 2.06	21.95 ± 2.70	26.36 ± 7.17	44.25 ± 12.50
C16:1	10.69 ± 1.23	11.15 ± 1.27	4.74 ± 0.51	3.23 ± 0.52	2.18 ± 0.85	3.40 ± 1.23
C18	8.89 ± 0.88	17.50 ± 1.30 ***	7.04 ± 1.15	11.97 ± 1.69 *	13.32 ± 2.87	30.36 ± 7.95
C18:1	50.49 ± 4.04	64.56 ± 4.04 *	31.34 ± 2.92	26.77 ± 3.66	32.95 ± 11.38	36.57 ± 10.67
C18:2	26.05 ± 1.69	25.31 ± 1.74	17.12 ± 1.62	13.94 ± 2.16	5.50 ± 2.13	6.91 ± 3.59
C18:3	2.04 ± 0.18	2.38 ± 0.27	1.16 ± 0.14	0.92 ± 0.16	0.24 ± 0.10	0.41 ± 0.20
C20	0.16 ± 0.02	0.43 ± 0.04 ****	0.28 ± 0.07	0.50 ± 0.07 *	1.02 ± 0.11	4.24 ± 0.66 ***
C20:1	2.65 ± 0.30	3.75 ± 0.30 *	2.79 ± 0.62	4.72 ± 0.80	9.37 ± 2.17	48.94 ± 12.63**
C20:4	5.76 ± 0.60	3.91 ± 0.47 *	3.56 ± 0.49	2.97 ± 0.33	4.01 ± 2.21	4.21 ± 2.10
C20:5	0.62 ± 0.06	0.35 ± 0.05 **	0.32 ± 0.05	0.23 ± 0.03	0.28 ± 0.16	0.21 ± 0.12
C22	0.04 ± 0.01	0.11 ± 0.01 ***	0.16 ± 0.03	0.26 ± 0.03	0.66 ± 0.06	1.94 ± 0.31 **
C22:1	0.26 ± 0.02	0.47 ± 0.04 ***	0.64 ± 0.16	0.97 ± 0.13	4.07 ± 0.96	14.11 ± 2.80 **
C22:6	1.70 ± 0.25	1.45 ± 0.09	1.21 ± 0.15	1.09 ± 0.12	2.24 ± 1.26	2.36 ± 0.95
C24	0.03 ± 0.01	0.10 ± 0.01 ***	0.15 ± 0.02	0.24 ± 0.02 *	0.46 ± 0.04	1.01 ± 0.20 *
C24:1	0.09 ± 0.01	0.19 ± 0.01 ****	0.26 ± 0.04	0.45 ± 0.07 *	1.45 ± 0.32	5.40 ± 1.20 **
Total	151.13 ± 10.92	199.69 ± 11.99 *	94.85 ± 9.34	96.65 ± 11.72	108.70 ± 32.92	219.44 ± 49.42
Saturated	50.49 ± 5.35	85.85 ± 5.16***	31.58 ± 3.92	41.26 ± 5.33	46.36 ± 11.95	96.72 ± 25.9
Unsaturated	100.64 ± 6.86	113.83 ± 7.52	63.26 ± 5.9	55.38 ± 7.42	62.33 ± 21.14	122.72 ± 31.1
LCFA (C14-C20)	149.01 ± 10.98	197.38 ± 11.96*	92.42 ± 9.04	93.64 ± 11.44	99.81 ± 30.39	194.62 ± 45.55
VLCFA (≥C22)	2.11 ± 0.23	2.3 ± 0.11	2.42 ± 0.34	3.00 ± 0.31	8.89 ± 2.58	24.82 ± 5.12*

Data are expressed as mean ± SEM. *p <0.05 , **p <0.01 , ***p <0.001 , ****p < 0.0001 measured by student's t-test (n=8). LCFA=long chain fatty acids; VLCFA=very long chain fatty acids.

Table 3 Total levels of other lipid species in intestine and feces (nmol/mg) assessed by HPLC-MS.

	Upper S.I. Control	Upper S.I. Cyp8b1-/-	Lower S.I. Control	Lower S.I. Cyp8b1-/-	L.I. Control	L.I. Cyp8b1-/-	Feces Control	Feces Cyp8b1-/-
MG	3.30 ± 0.14	4.12 ± 0.19 **	7.37 ± 0.35	6.32 ± 0.37	9.09 ± 0.94	6.65 ± 0.44 *	2.76 ± 0.96	9.63 ± 7.03
DG	11.86 ± 1.89	14.75 ± 1.15	18.51 ± 2.49	8.67 ± 1.74 **	8.86 ± 1.68	5.15 ± 0.44 *	1.67± 0.44	4.95 ± 2.08
TG	36.63 ± 6.01	59.34 ± 10.22	135.84 ± 20.79	70.68 ± 10.77 **	69.39 ± 10.73	31.72 ± 4.95 **	0.46 ± 0.13	2.10 ± 0.91
SM	12.70 ± 0.69	14.05 ± 0.92	8.36 ± 0.87	5.10 ± 0.70 **	4.48 ± 0.43	3.32 ± 0.32 *	0.06 ± 0.02	0.75 ± 0.51
PC	32.35 ± 2.26	34.46 ± 1.38	23.38 ± 1.89	15.38 ± 1.72 **	14.68 ± 1.56	11.82 ± 1.27	0.09 ± 0.05	0.44 ± 0.20
PE	11.80 ± 1.08	10.99 ± 0.58	0.36 ± 0.03	0.20 ± 0.04 **	0.19 ± 0.03	0.16 ± 0.02	0.01 ± 0.01	0.01 ± 0.01

Data are expressed as mean ± SEM. *p <0.05, **p <0.01 , ***p <0.001 , ****p < 0.0001 in $Cyp8b1^{-/-}$ versus controls, measured by student's t-test (n=8). Phosphatidylethanolamine [PE], phosphatidylcholine [PC], sphingomyelin [SM], tri- di and monoacylglycerol [TG, DG, MG].

MG group is composed of: MG 16:0, MG 16:1, MG 18:0, MG 18:1, MG 18:2, MG 18:3, MG 20:0, MG 20:2, MG 20:3, MG 20:4, MG 22:0, MG 22:3, MG 22:4, MG 22:5.
DG group is composed of: DG 28:0/14:0, DG 30:0/14:0, DG 30:1/14:0, DG 32:0/16:0, DG 32:1/16:0, DG 32:2/16:1, DG 34:0/16:0, DG 34:1/16:0, DG 34:2/16:0, DG 34:2/16:1, DG 36:0/18:0, DG 36:1/18:0, DG 36:2/18:0, DG 36:2/18:1, DG 36:3/18:1, DG 36:4/18:0, DG 38:2/18:0, DG 38:2/18:1, DG 38:3/18:0, DG 38:3/18:1, DG 38:4/18:0, DG 38:4/18:1, DG 40:4/18:0, DG 40:5/18:0, DG 40:5/18:1, DG 40:6/18:0, DG 40:6/18:1.
TG group is composed of: TG 48:0/16:0, TG 48:1/16:0, TG 50:0/16:0, TG 50:1/16:1, TG 50:2/16:1, TG 52:0/18:0, TG 52:1/18:0, TG 52:2/18:0, TG 52:3/18:1, TG 52:4/18:1, TG 52:5/20:4, TG 54:0/18:0, TG 54:1/18:0, TG 54:2/18:0, TG 54:3/18:0, TG 54:4/18:1, TG 54:4/20:4, TG 54:5/18:1, TG 54:6/18:1, TG 54:6/20:4, TG 54:7/18:1,TG 56:4/18:1, TG 56:4/20:4, TG 56:5/18:1, TG 56:8/20:4, TG 56:9/20:4, TG 58:7/20:4, TG 58:8/22:6, TG 58:9/22:6.
SM group is composed of: SM d18:1/16:0, SM d18:1/16:1, SM d18:1/18:0, SM d18:1/18:1, SM d18:1/20:0, SM d18:1/20:1, SM d18:1/22:0, SM d18:1/22:1, SM d18:1/24:0, SM d18:1/24:1.
PC group is composed of: PC 30:0, PC 32:0, PC 32:1, PC 34:0, PC 34:1, PC 34:2, PC 36:0, PC 36:1, PC 36:2, PC 36:3, PC 36:4, PC 38:1, PC 38:2, PC 38:3, PC 38:4, PC 38:5, PC 38:6, PC 40:4, PC 40:5, PC 40:6, PC 40:7.
PE group is composed of: PE 30:0, PE 32:0, PE 32:1, PE 34:0, PE 34:1, PE 34:2, PE 36:0, PE 36:1, PE 36:2, PE 36:3, PE 36:4, PE 38:0, PE 38:1, PE 38:2, PE 38:3, PE 38:4, PE 38:5, PE 38:6, PE 40:4, PE 40:5, PE 40:6.